Low-frequency electric microfield distributions in a plasma containing multiply-charged ions: Extended calculations*

Richard J. Tighe and C. F. Hooper, Jr.
Physics Department, University of Florida, Gainesville, Florida 32611
(Received 6 January 1977)

The formalism needed for the computation of electric microfield distributions in plasmas is extended as follows: (i) The perturbing ions and electrons in the plasma are allowed to have different kinetic temperatures; (ii) two species of perturbing ions, of charge Z_1 and Z_2, may be present in any given proportion. Computed results are presented graphically for parameter ranges which are of interest in the study of laser-produced plasmas.

I. INTRODUCTION

In a recent paper dealing with x-ray line broadening in hot, dense, laser-produced plasmas,[1] hereafter referred to as I, the formalism needed for the calculation of the appropriate electron-microfield distribution functions was outlined. Calculations were presented, in the static-ion approximation, for the low-frequency microfield distributions. These calculations made the following two assumptions: (i) the perturbing ions and electrons were in equilibrium with the same kinetic temperature; (ii) while multiply charged radiators were allowed, all of the perturbing ions were singly charged.

Since many plasmas currently being studied have different ion and electron temperatures,[2] and since a number of these also consider multiply charged ion perturbers,[3,4] it is useful to modify the previously developed theory by removing these two restrictions. A two-temperature formalism, the feasibility of which has already been demonstrated,[5] will be employed in this paper. Further, the formalism presented in I is modified to allow for two species of perturbing ions, having charges Z_1 and Z_2, in any given ratio.

In Sec. II the modifications of the theory previously developed are indicated. Section III contains a discussion of the results as presented in the figures. Conclusions are presented in Sec. IV.

II. FORMALISM

The calculations performed herein are based on a formalism developed in I. In this section we indicate the modifications necessary to convert that theory into one which allows for different ion and electron kinetic temperatures, and which also allows for two species of multiply charged ion perturbers. In the following, $P(\epsilon)$ is the probability distribution for the low-frequency electric microfield due to the static ions. The calculation of $P(\epsilon)$ involves the evaluation of the following sine transform:

$$P(\epsilon) = 2\pi^{-1}\epsilon \int_0^\infty T(L)\sin(\epsilon L)\, L\, dL\,, \tag{1}$$

where

$$T(L) = \exp[-\gamma L^2 + I_1(L) + I_2(L)]\,. \tag{2}$$

The forms of γ, $I_1(L)$, and $I_2(L)$ in the present work are different from those appearing in I. The appropriately modified expressions for (i) γ, (ii) $I_1(L)$, and (iii) $I_2(L)$ are as follows:

(i) γ: These expressions replace Eq. (5) in I:

$$\gamma = \tfrac{1}{4}a(\theta_i/\theta_e)[\alpha^2 - (1+u)]^{-2}B\,, \tag{3}$$

$$B = \alpha^5 u + 2[1-(1+u)^{3/2}]\alpha^4 + [2u+u^2]\alpha^3 - 4(1+u)[1-(1+u)^{1/2}]\alpha^2 - 3[u+u^2]\alpha + 2[(1+u)^2 - (1+u)^{3/2}]\,, \tag{4}$$

$$u = \frac{\theta_e}{\theta_i}\frac{Z_1^2 + RZ_2^2}{Z_1 + RZ_2}\,, \quad R = \frac{n_{z_2}}{n_{z_1}}\,, \quad \theta_e = kT_e\,, \quad \theta_i = kT_i\,. \tag{5}$$

(ii) $I_1(L)$: These expressions replace Eqs. (6)–(10) in I:

$$I_1(L) = I_{10}(L) + I_{01}(L)\,, \tag{6}$$

$$I_{10}(L) = \frac{3}{Z_1 + RZ_2}\int_0^\infty dx\, x^2 e^{Z_1 S(x)}\left[e^{-\beta Z_1 w_{10}(x)}\left(\frac{\sin[Z_1 LG(x)]}{Z_1 LG(x)} - 1\right) - \left(\frac{\sin[Z_1 Lq(x)]}{Z_1 Lq(x)} - 1\right)\right]\,, \tag{7}$$

$$I_{01}(L) = \frac{3R}{Z_1 + RZ_2}\int_0^\infty dx\, x^2 e^{Z_2 S(x)}\left[e^{-\beta Z_2 w_{10}(x)}\left(\frac{\sin[Z_2 LG(x)]}{Z_2 LG(x)} - 1\right) - \left(\frac{\sin[Z_2 Lq(x)]}{Z_2 Lq(x)} - 1\right)\right]\,, \tag{8}$$

$$\beta w_{10}(x) = \chi(\theta_e/\theta_i)(a^2/3x)e^{-\alpha a x}\,, \tag{9}$$

$$S(x) = \chi(\theta_e/\theta_i)(a^2/3x)[(\alpha^2-1)/(\alpha^2-(1+u))]\,(e^{-\alpha a x} - e^{-(1+u)^{1/2}\alpha x})\,, \tag{10}$$

$$q(x) = -\frac{\alpha^2-1}{\alpha^2-(1+u)}\left(\frac{1}{x^2}(e^{-\alpha a x} - e^{-(1+u)^{1/2}\alpha x}) + \frac{a}{x}\left[\alpha e^{-\alpha a x} - (1-u)^{1/2}\, e^{-(1+u)^{1/2}\alpha x}\right]\right)\,, \tag{11}$$

$$G(x) = q(x) + (1/x^2)e^{-\alpha a x}(1+\alpha a x)\,. \tag{12}$$

(iii) $I_2(L)$: These expressions replace Eq. (11) of I. We first define,

$$a' = (1+u)^{1/2}a\,. \tag{13}$$

a' is a modified plasma parameter. $I_2(L)$ is now given by

$$I_2(L) = I_{20}(L) + I_{02}(L) + I_{11}(L)\,, \tag{14}$$

$$I_{20}(L) = -Z_1^2(\theta_e/\theta_i)\left(\frac{1}{Z_1+RZ_2}\right)^2 3a^2 \sum_k (-1)^k(2k+1)A_{20}, \tag{15}$$

$$\begin{aligned} A_{20} = {} & \int_0^\infty x_2^{3/2} I_{k+1/2}(a'x_2)e^{Z_1 S(x_2)}[e^{-\beta Z_1 w_{10}(x_2)}\, j_k(Z_1 LG(x_2)) - j_k(Z_1 Lq(x_2))] \\ & \times \int_{x_2}^\infty x_1^{3/2} K_{k+1/2}(a'x_1)e^{Z_1 S(x_1)}[e^{-\beta Z_1 w_{10}(x_1)}\, j_k(Z_1 LG(x_1)) - j_k(Z_1 Lq(x_1))]\,dx_1\,dx_2 \\ & - \delta_{k,0}\int_0^\infty x_2^{3/2} I_{1/2}(a'x_2)e^{Z_1 S(x_2)}(e^{-\beta Z_1 w_{10}(x_2)} - 1)\int_{x_2}^\infty x_1^{3/2} K_{1/2}(a'x_1)e^{Z_1 S(x_1)}(e^{-\beta Z_1 w_{10}(x_1)} - 1)\,dx_1\,dx_2\,, \end{aligned} \tag{16}$$

$$I_{02}(L) = -Z_2^2(\theta_e/\theta_i)\left(\frac{R}{Z_1+RZ_2}\right)^2 3a^2 \sum_k (-1)^k(2k+1)A_{02}\,, \tag{17}$$

$$\begin{aligned} A_{02} = {} & \int_0^\infty x_2^{3/2}\, I_{k+1/2}(a'x_2)e^{Z_2 S(x_2)}[e^{-\beta Z_2 w_{10}(x_2)}\, j_k(Z_2 LG(x_2)) - j_k(Z_2 Lq(x_2))] \\ & \times \int_{x_2}^\infty x_1^{3/2} K_{k+1/2}(a'x_1)e^{Z_2 S(x_1)}[e^{-\beta Z_2 w_{10}(x_1)}\, j_k(Z_2 LG(x_1)) - j_k(Z_2 Lq(x_1))]\,dx_1\,dx_2 \\ & - \delta_{k,0}\int_0^\infty x_2^{3/2}\, I_{1/2}(a'x_2)e^{Z_2 S(x_2)}[e^{-\beta Z_2 w_{10}(x_2)} - 1]\int_{x_2}^\infty x_1^{3/2} K_{1/2}(a'x_1)e^{Z_2 S(x_1)}[e^{-\beta Z_2 w_{10}(x_1)} - 1]\,dx_1\,dx_2\,, \end{aligned} \tag{18}$$

$$I_{11}(L) = -Z_1 Z_2(\theta_e/\theta_i)R\left(\frac{1}{Z_1+RZ_2}\right)^2 3a^2 \sum_k (-1)^k(2k+1)A_{11}\,, \tag{19}$$

$$\begin{aligned} A_{11} = {} & \int_0^\infty x_2^{3/2} I_{k+1/2}(a'x_2)e^{Z_2 S(x_2)}[e^{-\beta Z_2 w_{10}(x_2)} j_k(Z_2 LG(x_2)) - j_k(Z_2 Lq(x_2))] \\ & \times \int_{x_2}^\infty x_1^{3/2} K_{k+1/2}(a'x_1)e^{Z_1 S(x_1)}[e^{-\beta Z_1 w_{10}(x_1)}\, j_k(Z_1 LG(x_1)) - j_k(Z_1 Lq(x_1))]\,dx_1\,dx_2 \\ & + \int_0^\infty x_2^{3/2} K_{k+1/2}(a'x_2)e^{Z_2 S(x_2)}[e^{-\beta Z_2 w_{10}(x_2)}\, j_k(Z_2 LG(x_2)) - j_k(Z_2 Lq(x_2))] \\ & \times \int_0^{x_2} x_1^{3/2} I_{k+1/2}(a'x_1)e^{Z_1 S(x_1)}[e^{-\beta Z_1 w_{10}(x_1)} j_k(Z_1 LG(x_1)) - j_k(Z_1 Lq(x_1))]\,dx_1\,dx_2 \\ & - \delta_{k,0}\int_0^\infty x_2^{3/2} I_{1/2}(a'x_2)e^{Z_2 S(x_2)}[e^{-\beta Z_2 w_{10}(x_2)} - 1]\int_{x_2}^\infty x_1^{3/2} K_{1/2}(a'x_1)e^{Z_1 S(x_1)}[e^{-\beta Z_1 w_{10}(x_1)} - 1]\,dx_1\,dx_2 \\ & - \delta_{k,0}\int_0^\infty x_2^{3/2} K_{1/2}(a'x_2)e^{Z_2 S(x_2)}[e^{-\beta Z_2 w_{10}(x_2)} - 1]\int_0^{x_2} x_1^{3/2} I_{1/2}(a'x_1)e^{Z_1 S(x_1)}[e^{-\beta Z_1 w_{10}(x_1)} - 1]\,dx_1\,dx_2\,. \end{aligned} \tag{20}$$

III. RESULTS

In Figs. 1–6, we present the results of the two-temperature calculations. In all of these cases $R = 0.0$, which implies that only one perturbing ion species (of charge Z_1) is present. Figures 1 and 2 show the behavior of Ne-H microfield distributions under variation of the parameter T_R. (The notation Ne-H refers to hydrogen-like neon radiators immersed in a hydrogen or deuterium-

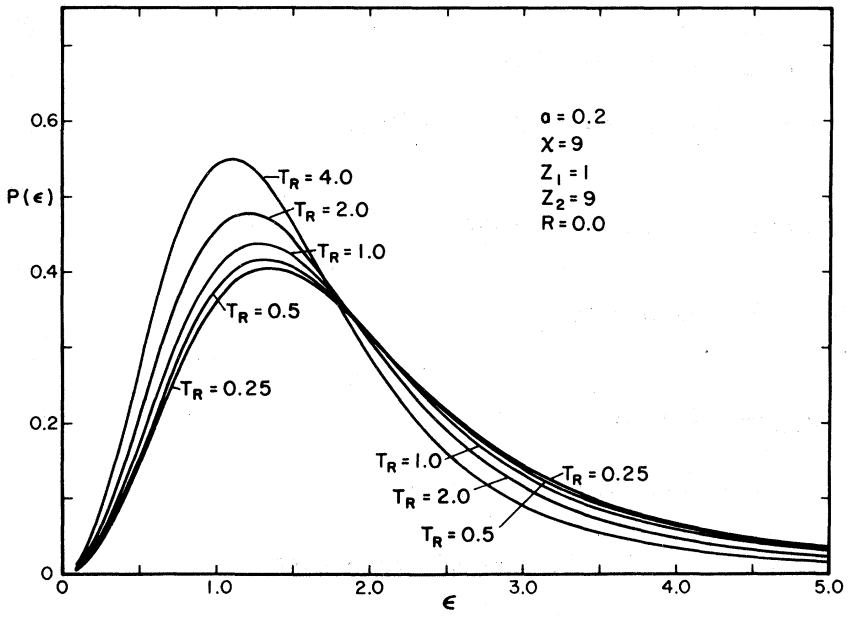

FIG. 1. Electric microfield distribution function $P(\epsilon)$ at a point having a charge of +9. $a=0.2$. Perturbing ions have a charge of +1. ϵ is in units of $\epsilon_0(=e/r_0^2)$ and $a=r_0/\lambda_D$. Tables corresponding to these curves are available upon request.

tritium plasma.) Figures 3 and 4 show Ar-H; Figs. 5 and 6 show Al-Al microfield distributions. In these figures T_R is given by

$$T_R = kT_e/kT_i = \theta_e/\theta_i \,. \tag{21}$$

As the value of the parameter T_R is increased, in all cases, the microfield distribution function peaks shift to lower values of ϵ. This behavior might be anticipated from the form of the following relation:

$$a' = (1+u)^{1/2} a \,, \tag{22}$$

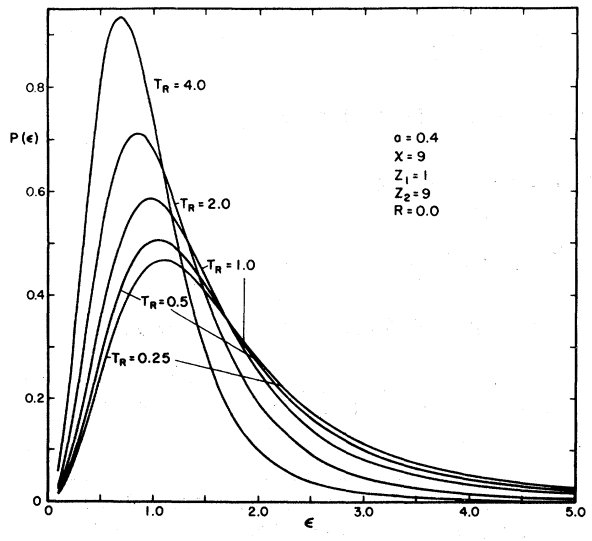

FIG. 2. Electric microfield distribution function $P(\epsilon)$ at a point having a charge of +9. $a=0.4$. Tables corresponding to these curves are available upon request.

where, if $R=0.0$,

$$u = (\theta_e/\theta_i) Z_1 = T_R Z_1 \,. \tag{23}$$

Thus, if we regard a' as a modified plasma parameter, we see that as the value of T_R is increased, the result is an effective increase in the a value. A direct comparison of Figs. 1–6 with Figs. 1 and 2 of I indicates that when the value of T_R is increased, the present curves indeed exhibit behavior similar to that noted previously when the a value was increased. While the dependence on T_R is obviously strong in all cases considered, the analytic form of this dependence is extremely complicated and difficult to assess.

To see more clearly the effect of the $(1+u)^{1/2}$ factor, let us consider the following:

$$a' = (1+u)^{1/2} a = (1+u)^{1/2} r_0/\lambda_D = r_0/\lambda_D' \,, \tag{24}$$

where

$$\lambda_D' = \left(\frac{4\pi n e^2 (1+u)}{\theta_e} \right)^{-1/2} . \tag{25}$$

The definition of u is given in Eq. (5); we now write it in the form

$$u = \frac{\theta_e}{\theta_i} \frac{N_1 Z_1^2 + N_2 Z_2^2}{N_1 Z_1 + N_2 Z_2} = \frac{\theta_e}{\theta_i} \frac{n_1 Z_1 + n_2 Z_2^2}{n} \,. \tag{26}$$

The second step in Eq. (26) results from the overall charge neutrality of the plasma. Inserting this result into Eq. (25) we obtain

$$\lambda_D' = \left[4\pi e^2 \left(\frac{n}{\theta_e} + \frac{n_1 Z_1^2 + n_2 Z_2^2}{\theta_i} \right) \right]^{-1/2} . \tag{27}$$

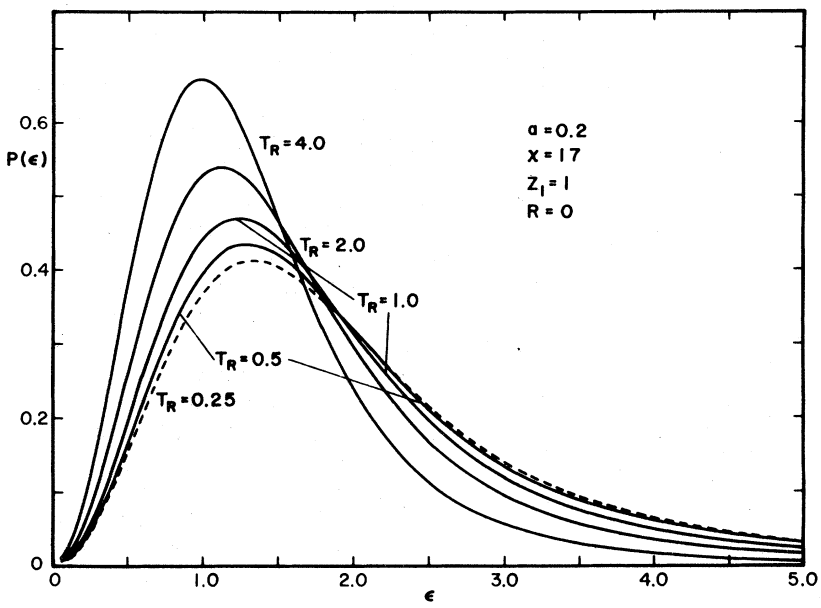

FIG. 3. Electric microfield distribution function $P(\epsilon)$ at a point having a charge of +17. $a = 0.2$. Perturbing ions have a charge of +1. Tables corresponding to these curves are available upon request.

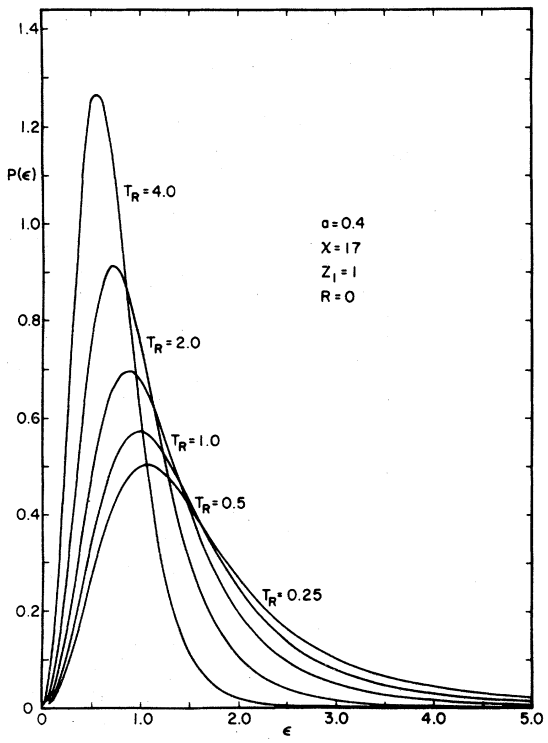

FIG. 4. Electric microfield distribution function $P(\epsilon)$ at a point having a charge of +17. $a = 0.4$. Tables corresponding to these curves are available upon request.

This equation is a generalization of Eq. (19) in Ref. 6.

In our computations, we regard T_e and n (the electron number density) as fixed by the parameter a. This means that, for a given value of a, an increase in T_R is accompanied by a decrease in the ion temperature. Equations (24) and (27) give the explicit dependence of a' on the ion tem-

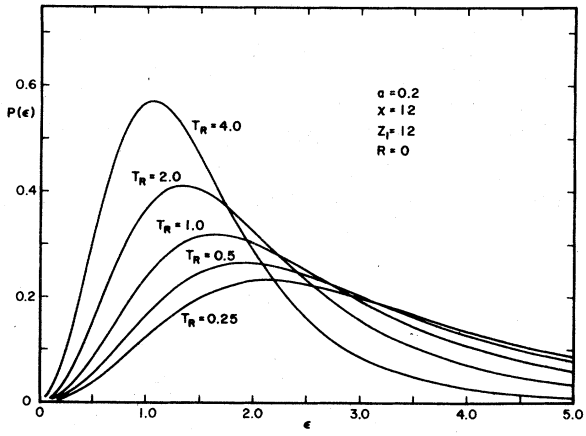

FIG. 5. Electric microfield distribution function $P(\epsilon)$ at a point having a charge of +12. $a = 0.2$. Perturbing ions have a charge of +12. Tables corresponding to these curves are available upon request.

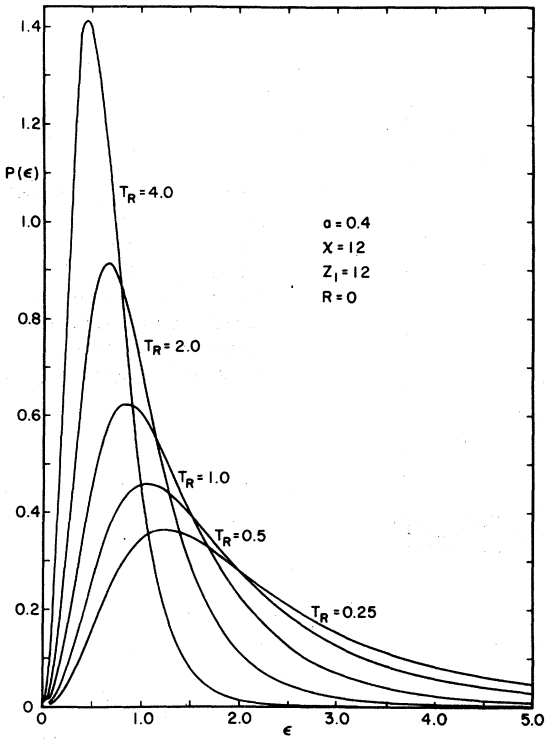

FIG. 6. Electric microfield distribution function $P(\epsilon)$ at a point having a charge of +12. $a = 0.4$. Tables corresponding to these curves are available upon request.

perature. In addition, this equation suggests that the shift of the microfield peaks might be due to increased importance of ion correlations as ion temperature is lowered. This correlation effect is especially apparent in Figs. 4 and 6. Looking at these figures we see that, as T_R takes higher values (ion temperature decreases), the Al microfield distributions peak at smaller field values than do the argon distributions. This is to be expected since interparticle correlations are stronger in the Al-Al system than in the Ar-H system. However, as T_R decreases (ion temperature increases), the figures indicate that stronger fields are more probable in the Al plasma. This is due to weakened correlations; the average interactions will be stronger in the Al-Al system in the Ar-H system.

In Figs. 7–10, we present the results of computations in which T_R is set equal to unity and the parameter R is varied; R is the ratio of the density of charge-Z_2 perturbers to the density of charge-Z_1 perturbers. $R = 0.0$ (∞) corresponds to the case where the perturbers are all of charge Z_1 (Z_2). (We specify that $Z_2 > Z_1$.) The function u

$$u(T_R = 1) = \frac{Z_1^2 + RZ_2^2}{Z_1 + RZ_2}$$

varies smoothly from a value of Z_1 to a value of Z_2 as R goes from 0.0 to ∞. Because of this we might expect that when the perturbing ions have Z_1 and Z_2 nearly equal, the variation of R causes very little change in $P(\epsilon)$. Indeed, this is the case for Al microfields when $Z_1 = 12$ and $Z_2 = 11$. For this reason we omit the figures showing the R variation calculations for the Al system.

The most noticeable effect of an R variation occurs when Z_1 and Z_2 are very different (Figs. 7–10). Furthermore, it should be noted that for very different Z_1 and Z_2, most of the variation of $P(\epsilon)$ occurs between the range of $R = 0.0$ and R

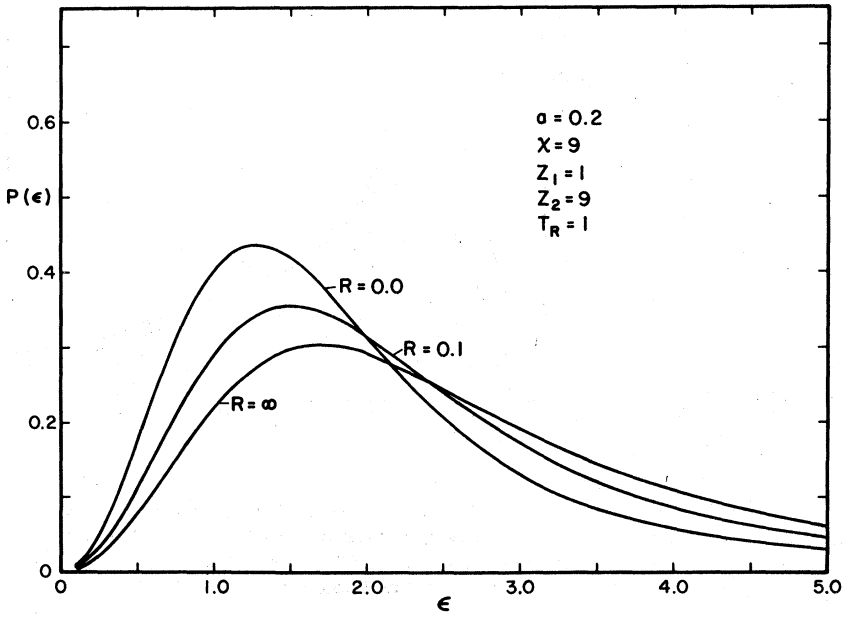

FIG. 7. Electric microfield distribution function $P(\epsilon)$ at a point having a charge of +9. $a = 0.2$. Perturbing ions have charges +1 and +9. Tables corresponding to these curves are available upon request.

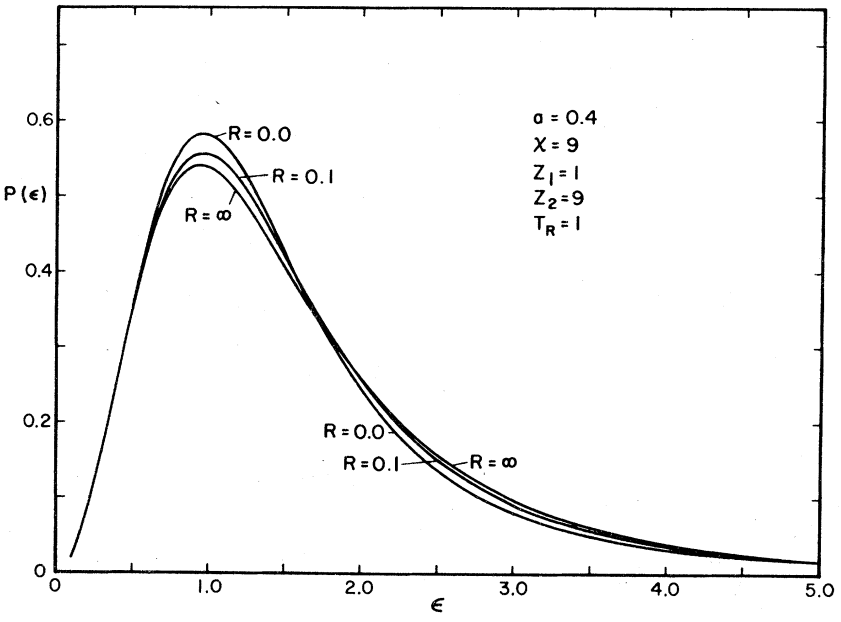

FIG. 8. Electric microfield distribution function $P(\epsilon)$ at a point having a charge of +9. $a = 0.4$. Tables corresponding to these curves are available upon request.

$= 0.1$. This indicates that the interactions involving ions with charge Z_2 tend to saturate and overwhelm the interactions involving Z_1 (for $Z_2 > Z_1$).

IV. CONCLUSIONS

In I microfield distributions were parametrized by a and χ. In this paper we have added four more parameters: $P(\epsilon)$ is now parametrized by a, χ, Z_1, Z_2, R, T_R.

The $P(\epsilon)$ curves show strong dependence on the parameter T_R. Knowledge of this dependence should greatly enhance the usefulness of x-ray line broadening as a diagnostic for laser-produced plasmas. Also, for small a values, there is a marked sensitivity to small amounts of impurity concentration which may prove to be of interest. Laser-produced plasmas tend to be of short

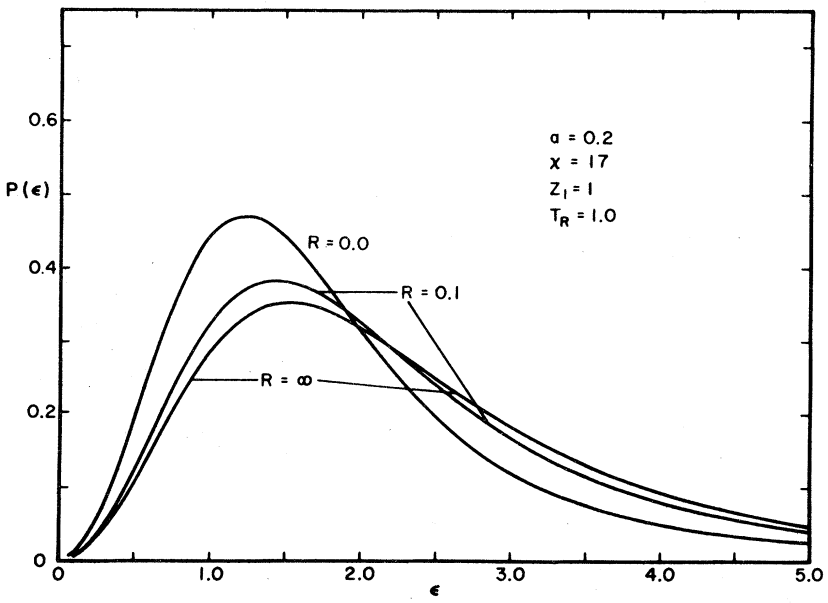

FIG. 9. Electric microfield distribution function $P(\epsilon)$ at a point having a charge of +17. $a = 0.2$. Perturbing ions have charges +1 and +17. Tables corresponding to these curves are available upon request.

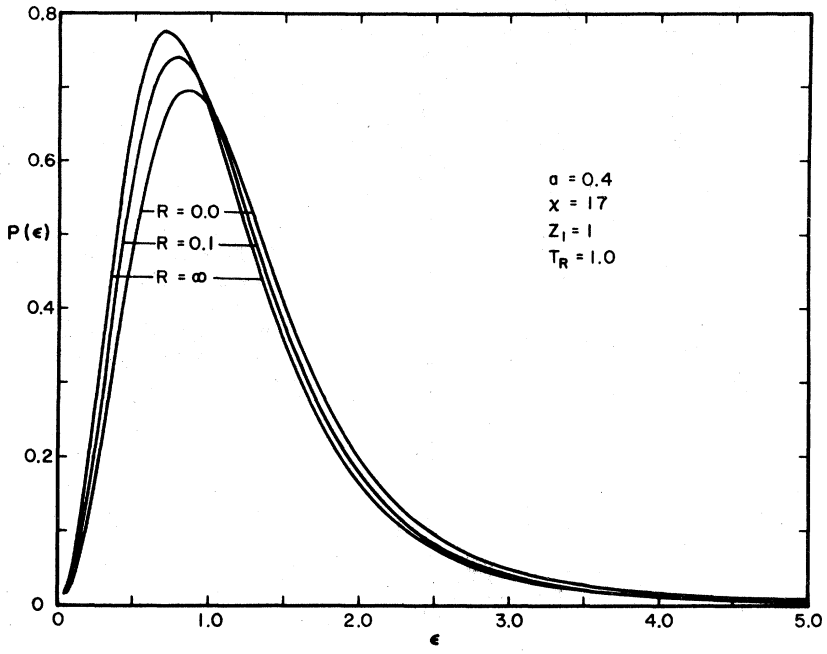

FIG. 10. Electric microfield distribution function $P(\epsilon)$ at a point having a charge of +17. $a = 0.4$. Tables corresponding to these curves are available upon request.

duration—characterized by rapid variation of the parameters mentioned above. This theory offers the capability of incorporating a knowledge of the time dependence of a, R, T_R, etc. into the computation of time-averaged spectral line profiles emitted by transient plasmas.

ACKNOWLEDGMENT

One of us (R.J.T.) would like to thank Dr. Robert L. Coldwell (University of Florida) for several computer codes, as well as a number of helpful discussions.

*Work supported in part by the Lawrence Livermore Laboratory, ERDA, and the Northwest Regional Data Center of the State University System of Florida.

[1]R. J. Tighe and C. F. Hooper, Jr., Phys. Rev. A 14, 1514 (1976).

[2]G. F. Chapline, H. E. DeWitt, and C. F. Hooper, Jr., UCRL Report No. 76272, 1974 (unpublished).

[3]J. C. Weisheit, C. B. Tarter, J. H. Scofield, and L. M. Richards, J. Quant. Spectrosc. Radiat. Transfer 16, 659 (1976).

[4]H. R. Griem and P. C. Kepple (unpublished).

[5]J. T. O'Brien and C. F. Hooper, Jr., Phys. Rev. A 5, 867 (1972).

[6]B. Mozer and M. Baranger, Phys. Rev. 118, 626 (1960).